

THE COHESIVE SEGMENTS METHOD FOR THE SIMULATION OF FRACTURE

Joris J.C. Remmers¹, René de Borst^{1,2} and Alan Needleman³

¹ Faculty of Aerospace Engineering, Delft University of Technology, NL-2600 GB Delft, The Netherlands.

² LaMCoS - UMR CNRS 5514, I.N.S.A. de Lyon, F-69021 Villeurbanne, France.

³ Division of Engineering, Brown University, Providence, RI, 02912, U.S.A.

ABSTRACT

The cohesive segments method is briefly described. This method, which uses the partition-of-unity property of finite element shape functions, allows for the simulation of discontinuous crack growth in a mesh independent way. The potential of the method in both quasi-static and dynamic simulations is illustrated by two examples.

1 INTRODUCTION

Linear elastic fracture mechanics applies when there is a crack-like flaw in an otherwise linear elastic solid and the singularity associated with that flaw is characterised by a non-vanishing energy release rate. For example, classical linear elastic fracture mechanics concepts do not apply for dynamic crack growth in a brittle solid in the intersonic regime. The fracture and any dissipative processes must also remain confined to a small region in the vicinity of the crack tip. If these conditions are not met, linear elastic fracture mechanics concepts do not apply and another fracture framework is needed.

When the region in which the separation and dissipative process take place is not small compared to a structural dimension, but any nonlinearity is confined to a surface emanating from a classical crack tip (i.e. one with a non-vanishing energy release rate), cohesive zone models which were introduced by Barenblatt [1] and Dugdale [2] can be applied. Subsequently, the cohesive zone approach was extended by Hillerborg *et al.* [3] and Needleman [4] to circumstances where: (i) an initial crack-like flaw need not be present or, if one is present, it need not be associated with a non-vanishing energy release rate; and (ii) non-linear deformation behaviour (but not separation) may occur over an extended volume. In this view of cohesive modelling, the continuum is characterised by two constitutive relations: a volumetric relation that relates stress and strain and a cohesive relation that relates traction to separation across a set of cohesive surfaces. Thus, for a cohesive formulation to apply, whatever fracture mechanism is occurring, it must be appropriate to idealise it as taking place over a surface of negligible thickness.

When the crack path is known in advance, either from experimental evidence, or because of the structure of the material (such as in laminated composites), cohesive-zone models have been used with considerable success. In those cases, the mesh can be constructed such that the crack path *a priori* coincides with the element boundaries. The crack itself is modelled by interface elements, which are equipped with a cohesive constitutive relation that consists of two parts: a finite stiffness to model a perfect bond prior to cracking and a softening part that describes the cracking behaviour. Introducing a finite stiffness prior to the onset of cracking changes the compliance of the structure

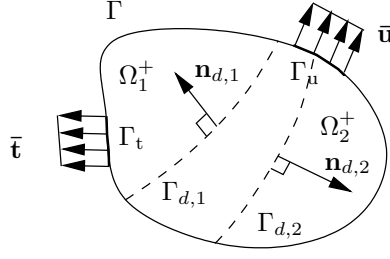


Figure 1: Domain crossed by two discontinuities $\Gamma_{d,1}$ and $\Gamma_{d,2}$.

and gives rise to deformations in the interface before crack initiation. Furthermore, in dynamic analyses, it will cause a change in the wave speeds. Although these effects can be limited by choosing a sufficiently high initial stiffness, other numerical deficiencies remain. For example, depending on the chosen spatial integration scheme, a high initial stiffness can lead to spurious traction oscillations, which may cause erroneous crack patterns, e.g. [5].

In many cases however, the trajectory of a crack is not known beforehand and, more important, crack growth is not a continuous process, e.g. in heterogeneous materials such as concrete. Here, the presence of particles of different sizes and stiffnesses leads to a complex stress field where new cracks nucleate and existing cracks coalesce. A similar behaviour can be observed in dynamic fracture. When the crack speed approaches the Rayleigh wave speed of the material, the fracture process is characterised by intermittent crack propagation and micro-crack nucleation or branching in the vicinity of the main crack tip.

In order to model such fracture mechanisms, Xu and Needleman [6] have inserted interface elements equipped with a cohesive-zone model between *all* continuum elements. Although such analyses provide much insight, they suffer from a certain mesh bias, since the direction of crack propagation is not entirely free, but is restricted to interelement boundaries [7].

In principle, most of the numerical problems are overcome by inserting the cohesive zones directly into the continuum elements by exploiting the partition-of-unity property of finite element shape functions [8, 9, 10]. Here, cohesive zones can be extended during the simulation, in any direction, irrespective of the structure of the underlying finite element mesh. As a further extension one can define *cohesive segments* that can arise at arbitrary locations and in arbitrary directions and allow for the resolution of complex crack patterns including crack nucleation at multiple locations, followed by growth and coalescence [11].

2 THE COHESIVE SEGMENTS METHOD

A key feature of the cohesive segments approach is the possible emergence of multiple cohesive segments in a domain. Consider a domain Ω which contains m discontinuities $\Gamma_{d,j}$, $j = 1, \dots, m$, see Figure 1. Each discontinuity splits the domain in two parts, denoted as Ω_j^- and Ω_j^+ , such that $\Omega_j^- \cup \Omega_j^+ = \Omega$. The displacement field can be written as the sum of $m + 1$ continuous displacement fields $\bar{\mathbf{u}}$ and $\tilde{\mathbf{u}}_j$ [12]:

$$\mathbf{u} = \bar{\mathbf{u}} + \sum_{j=1}^m \mathcal{H}_{\Gamma_{d,j}} \tilde{\mathbf{u}}_j \quad (1)$$

where $\mathcal{H}_{\Gamma_{d,j}}$ denotes the Heaviside step function which is equal to 1 when the material point is in Ω_j^+ and equals 0 otherwise. Restricting attention to small displacement gradients, the strain field

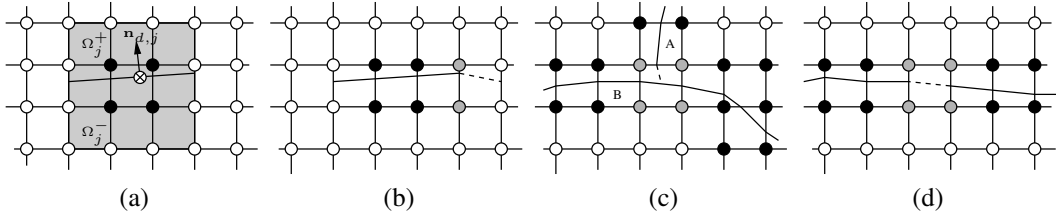


Figure 2: (a) A single cohesive segment in a quadrilateral mesh. The segment passes through an integration point (\otimes) where the fracture criterion is violated. The solid nodes contain additional degrees of freedom that determine the magnitude of the displacement jump. The gray shade denotes the elements that are influenced by the cohesive segment. (b) A cohesive segment is extended into a new element (dashed line). The gray nodes contain degrees of freedom that have just been added to support the extension of the cohesive segment. (c) Interaction of two cohesive segments. Segment A is extended (dashed line) until it touches segment B. Since this can be regarded as a free edge, there will be no crack tip for segment A. (d) Two segments are connected (dashed line).

follows by differentiation of (1):

$$\boldsymbol{\epsilon} = \nabla^s \bar{\mathbf{u}} + \sum_{j=1}^m (\mathcal{H}_{\Gamma_{d,j}} \nabla^s \tilde{\mathbf{u}}_j + \delta_{\Gamma_{d,j}} (\tilde{\mathbf{u}}_j \otimes \mathbf{n}_{\Gamma_{d,j}})^s) \quad (2)$$

where $\delta_{\Gamma_{d,j}}$ denotes the Dirac delta function placed at the j^{th} discontinuity $\Gamma_{d,j}$ and the superscript s denotes the symmetric part of the tensor. Note that the strain field is unbounded at the discontinuities $\Gamma_{d,j}$. Here, the magnitude of the displacement jump is taken as the governing kinematic parameter:

$$\mathbf{v}_j = \tilde{\mathbf{u}}|_{\Gamma_{d,j}} \quad (3)$$

The equilibrium equations in weak form are obtained by following a standard Bubnov-Galerkin procedure. These equations can be discretised by using the partition-of-unity property of finite element shape functions [8] as described in Remmers *et al.* [11].

Implementation

When the criterion for the initiation of decohesion is met (currently, a principal stress criterion is used) a cohesive segment is inserted through the integration point. In the applications so far, its direction has been taken to be orthogonal to the direction of the major principal stress. The segment is taken to extend through the element to which the integration point belongs and into the neighbouring elements, see Figure 2(a). The magnitude of the displacement jump is determined by a set of additional degrees of freedom which are added to all nodes whose support is crossed by the cohesive segment. The nodes of the element boundary that is touched by one of the two tips of the cohesive segment are not enhanced in order to ensure a zero opening at these tips [10]. Subsequently, the evolution of the separation of the cohesive segment is governed by a decohesion constitutive relation. When the criterion for the initiation is met at one of the two tips, the cohesive segment is extended into a new element, as demonstrated in Figure 2(b). The extension is straight within the element, but does not necessarily have to be aligned with previous parts of the segment, so that curved crack paths can be simulated.

Each cohesive segment is supported by its own set of additional degrees of freedom. When two segments meet within a single element, the nodes that support the element are enhanced twice, once

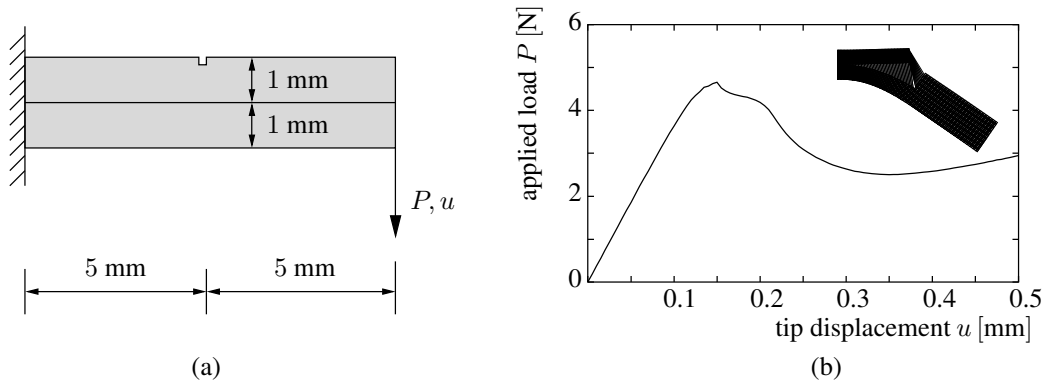


Figure 3: (a) Geometry of the double cantilever beam test. (b) Load displacement curve. In the inset, the final deformation of the specimen is shown (amplification factor 100.0).

for each cohesive segment. In the situation depicted in Figure 2(c), segment A is only extended until it touches segment B, which can be regarded as a free edge. This implies that there is no crack tip, so that all four nodes of the element are enhanced. A special case is shown in Figure 2(d). When two segments approach as shown in this figure, they are simply joined.

Because the crack is not taken as a single entity *a priori* in the cohesive segments approach, the method can equally well simulate distributed cracking which frequently occurs in a heterogeneous solid. Thus, the cohesive segments approach embraces both extremes, distributed cracking with crack nucleation, growth and eventual coalescence at multiple locations as well as the initiation and propagation of a single dominant crack without requiring special assumptions. What is needed is to specify the conditions for crack nucleation and for the crack propagation direction, and a decohesion relation at the crack.

3 NUMERICAL EXAMPLES

The performance of the cohesive segments method is demonstrated by means of two examples. The first example is a quasi-static analysis of a combination of fracture mechanisms in a double cantilever beam, the second example describes the analysis of dynamic shear fracture.

Double cantilever beam

Consider the double cantilever beam with a small notch as shown in Figure 3(a). The beam is subjected to bending. The two layers of the beam are composed of isotropic linear elastic materials and have identical elastic properties: Young's modulus $E = 20.0$ GPa and Poisson's ratio $\nu = 0.2$. The cohesive tensile stress of the material is $f_t^{\text{lay}} = 2.5$ MPa, the work of separation is $\mathcal{G}_c^{\text{lay}} = 40.0$ N/m. It is assumed that the fracture mode is purely mode-I. The adhesive that bonds the two layers is modelled with a *mixed mode* delamination model with a non-zero compliance prior to cracking [6] with fracture toughness $\mathcal{G}_c^{\text{adh}} = 10.0$ N/m and ultimate normal and shear traction $t_{n,\text{max}} = t_{s,\text{max}} = 1.0$ MPa.

The specimen is analysed with a mesh having 99×21 elements. The notch is simulated by removing a single element from the mesh. The interface between the two layers is modelled by a cohesive segment, which is added to the mesh beforehand. This implies that one part of the element that is crossed by this segment belongs to the top layer of the double-cantilever beam, the other part belongs to the bottom layer.

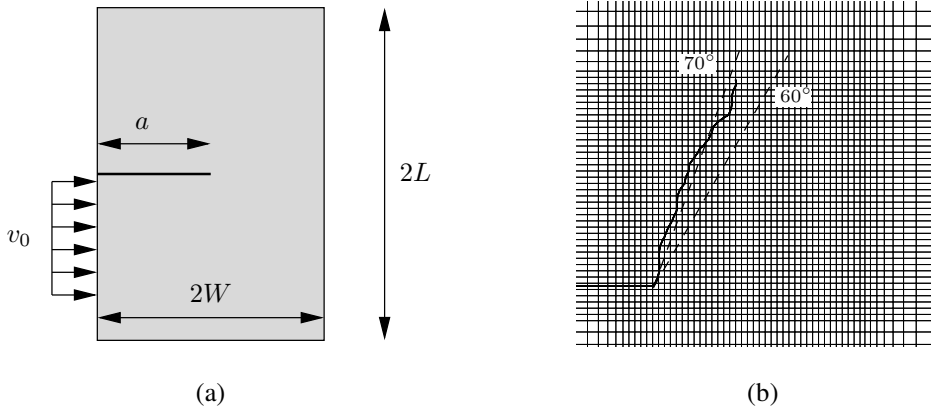


Figure 4: (a) Geometry and loading conditions for the specimen in the dynamic shear fracture test. (b) The Position of the crack (bold line) at $t = 5.0$ ms. The dashed lines are the projections of straight cracks at angles of 60° and 70° .

The tip displacement u is plotted against the applied load in Figure 3(b). When the applied load is equal to $F \approx 2.4$ N, a crack nucleates at the notch in the top layer. A new cohesive segment is added to the finite element model. Upon further loading, the crack propagates towards the interface. At this point the top layer has completely debonded and the interface is now loaded in nearly pure mode-II. When the shear tractions in the interface exceed the decohesion strength, the two layers start to debond. The highly distorted elements in the inset of Figure 3(b) contain the displacement jumps \mathbf{v}_j that govern the open cracks. The actual deformation of the material modelled by these elements is of the same order of magnitude as the deformation in the surrounding elements.

Dynamic shear fracture

The dynamic shear failure test is a classical example of fast crack growth in a homogeneous solid and has been the subject of many studies, e.g. [13, 14]. Under high impact loads, a crack that is subjected to a mode II load propagates at an angle of approximately 60° to 70° with respect to the initial crack.

Various calculations were carried out for the configuration shown in Figure 4(a). In some calculations numerical instabilities were encountered, while in other calculations there were difficulties associated with resolving near crack tip fields with the mesh used. These issues are being investigated. Nevertheless, good results were obtained for a specimen that has dimensions $L = 0.003$ m and $W = 0.0015$ m and has an initial crack with length $a = 0.0015$ mm. It is made of a homogeneous material with Young's modulus $3.24 \cdot 10^9$ N/m², Poisson's ratio 0.35 and density $\rho = 1190.0$ kg/m³. The corresponding dilatational, shear and Rayleigh wave speeds are $c_d = 2090$ m/s, $c_s = 1004$ m/s and $c_R = 938$ m/s. The ultimate normal traction of the material is equal to $100.0 \cdot 10^6$ N/m² and the fracture toughness is 700 N/m. The lower half of the specimen is subjected to an impulse load which is modelled as a prescribed velocity with magnitude $v_0 = 10$ m/s and a rise time $t_r = 0.1$ μ s.

The specimen is modelled with linear quadrilateral elements. In the region around the crack tip, the mesh is locally refined and the length of the elements is $l_e = 15.0$ μ m. The time increment is set to $\Delta t = 1.0 \cdot 10^{-10}$ s. At the start of the simulation, the model has 11587 degrees of freedom. In this specific example, crack nucleation away from the main crack tip is not taken into account.

As can be seen in Figure 4(b), the crack propagates roughly at an angle around 70° , which is in agreement with previous observations [13]. The small fluctuations in the path are most likely caused

by stress waves reflections.

4 CONCLUDING REMARKS

Cohesive–zone models constitute a powerful approach to analyse fracture, in particular for heterogeneous materials and for dynamic fracture. The bulk and cohesive constitutive relations together with appropriate balance laws and boundary (and initial) conditions completely specify the problem. Fracture, if it takes place, emerges as a natural outcome of the deformation process.

The partition-of-unity property of finite element shape functions enables a natural implementation of cohesive–zone models, unbiased by the initial mesh design. The formulation can be used in a wide variety of numerical applications, such as the cohesive segments method, where cohesive surfaces of a finite size can be defined, which can be placed at arbitrary locations and in arbitrary directions. The issues related to the numerical stability and the application of the method to discontinuous crack growth in dynamic simulations will be addressed as the development of the method proceeds.

REFERENCES

- [1] Barenblatt, G.I., The mathematical theory of equilibrium cracks in brittle fracture, *Advances in Applied Mechanics*, **7**, 55–129, 1962.
- [2] Dugdale, D.S., Yielding of steel sheets containing slits, *Journal of the Mechanics and Physics of Solids*, **8**, 100–108, 1960.
- [3] Hillerborg, A., Modeer, M. and Petersson, P.E., Analysis of crack formation and crack growth in concrete by means of fracture mechanics and finite elements, *Cement and Concrete Research*, **6**, 773–782, 1976.
- [4] Needleman, A., A continuum model for void nucleation by inclusion debonding, *Journal of Applied Mechanics*, **54**, 525–531, 1987.
- [5] Schellekens, J.C.J., de Borst, R., On the numerical integration of interface elements, *International Journal for Numerical Methods in Engineering*, **36**, 43–66, 1992.
- [6] Xu, X.P. and Needleman, A., Numerical simulations of fast crack growth in brittle solids, *Journal of the Mechanics and Physics of Solids*, **42**, 1397–1434, 1994.
- [7] Tijssens, M.G.A., Sluys, L.J. and van der Giessen, E., Numerical simulation of quasi-brittle fracture using damaging cohesive surfaces, *European Journal of Mechanics: A/Solids*, **19**, 761–779, 2000.
- [8] Babuska, I. and Melenk, J.M., The partition of unity method, *International Journal for Numerical Methods in Engineering*, **40**, 727–758, 1997.
- [9] Moës, N., Dolbow, J. and Belytschko, T., A finite element method for crack growth without remeshing, *International Journal for Numerical Methods in Engineering*, **46**, 131–150, 1999.
- [10] Wells, G.N. and Sluys, L.J., A new method for modeling cohesive cracks using finite elements, *International Journal for Numerical Methods in Engineering*, **50**, 2667–2682, 2001.
- [11] Remmers, J.J.C., de Borst, R., Needleman, A., A cohesive segments method for the simulation of crack growth, *Computational Mechanics*, **31**, 69–77, 2003.
- [12] Daux, C., Moës, N., Dolbow, J., Sukumar, N. and Belytschko, T., Arbitrary branched and intersecting cracks with the extended finite element method, *International Journal for Numerical Methods in Engineering*, **48**, 1741–1760, 2000.
- [13] Kalthoff J.K. and Winkler S., Failure mode transition at high rates of loading. *Proceedings of the International Conference on Impact Loading and Dynamic Behaviour of Materials*, Chiem C.Y., Kunze H.D. and Meyer L.W. eds., 43-56, Deutsche Gesellschaft für Metallkunde, 1988.
- [14] Needleman A. and Tvergaard V., Analysis of a brittle-ductile transition under dynamic shear loading *International Journal of Solids and Structures*, **32**, 2571–2590, 1995.